

Synthesis of Co Nanoparticles by Pulsed Laser Irradiation of Cobalt Carbonyl in Organic Solution

Ian Robinson,[†] Martin Volk,^{‡,‡} Le D Tung,^{||} Gabriel Caruntu,[⊥] Nicola Kay,[†] and Nguyen TK Thanh^{*,#,\#}

Department of Chemistry, University of Liverpool, Crown Street, Liverpool L69 7ZD, U.K., Surface Science Research Centre, University of Liverpool, Oxford Street, Liverpool L69 3BX, U.K., Department of Physics, University of Liverpool, Crown Street, Liverpool L69 7ZE, U.K., Advanced Materials Research Institute, College of Sciences, University of New Orleans, 2000 Lakeshore Drive, New Orleans, Louisiana 70148, The Davy-Faraday Research Laboratory, The Royal Institution of Great Britain, 21 Albemarle Street, London W1S 4BS, U.K., and Department of Physics & Astronomy, University College London, Gower Street, London WC1E 6BT, U.K.

Received: February 17, 2009; Revised Manuscript Received: April 21, 2009

Interest in producing magnetic nanoparticles with controllable sizes has led to the development of new synthesis methods. In this article, we report the synthesis of sub 4 nm cobalt nanoparticles by using pulsed laser irradiation to decompose cobalt carbonyl in a solution of stabilizing ligands. The physical characteristics of the synthesized nanoparticles were determined by transmission electron microscopy, powder X-ray diffractometry, and SQUID magnetometry. It was possible to control the size of the synthesized nanoparticles by varying the reaction conditions such as the ligand concentration and the wavelength of light used. The formation mechanism of the nanoparticles was also investigated by changing these conditions. It is possible that this technique could be applied to the synthesis of a variety of nanomaterials with potential applications such as biomedicine, catalysis, and water purification.

Introduction

Interest in magnetic nanoparticles (NPs) has grown rapidly in recent years due to their diverse potential applications in biomedicine and as novel materials for engineering and devices, which arise from their unique physical^{1–5} and chemical^{6–9} properties. These properties depend on the size and shape of the magnetic NPs and on the nature of the ligands bound to their surface. In particular, magnetic NPs have many potential biomedical applications such as magnetic resonance imaging (MRI), targeted drug delivery, hyperthermia treatment of solid tumors, and cell separation.^{10,11} There is also potential for these NPs to be used in nonmedical applications such as catalysis¹² and water purification.¹³

For use in these applications, the magnetic NPs need to be biocompatible and biodegradable, and hence, iron oxide NPs have been developed for these purposes. However, one drawback of using iron oxide is the need for relatively large NPs due to their relatively low magnetic susceptibility. The use of larger NPs can result in the increased chance of causing an embolism and damage to blood vessels.¹⁴ It is therefore desirable to use Co NPs because of their high saturation magnetization and strong response to an external magnetic field that allow smaller NPs to be used. There is some concern about the use of Co in biomedical applications as its toxicological assessments have not been thoroughly studied. However, if the NPs have a

diameter of less than 8 nm, they can be filtered through the glomeruli of the kidney and can therefore be rapidly cleared from the body.¹⁵ The renal clearance of metallic NPs is enhanced if they have a cationic or zwitterionic surface charge.¹⁵ The surface of Co NPs can be modified postsynthesis by ligand exchange techniques to allow them to be well dispersed in water for use in biological systems.¹⁶

Several methods have been developed for the synthesis of magnetic NPs including thermal decomposition of organometallic compounds such as dicobalt octacarbonyl [Co₂(CO)₈] at high temperature in organic solvent and in the presence of suitable stabilizers.^{17,18} In our group, NPs have also been synthesized that are coated with hydrophilic polymers or peptides as ligands, which allows the NPs to be dispersed in aqueous solution.^{18–20} Another method to synthesize Co NPs is to use a laser to induce the decomposition of Co₂(CO)₈ vapor produced by evaporation of the precursor.²¹ This laser evaporation method has been used to produce a variety of nanosized materials such as an FeCo alloy and silica coated iron oxide NPs.^{22–24} Ultraviolet irradiation of a cobalt(II) acetate solution has also been used to synthesize Co NPs which have certain morphologies depending upon the experimental parameters.²⁵ For any particular application there is an optimal size of NPs. For instance, biomedical applications require NPs with a size comparable to biomolecules,²⁶ and indeed, very small NPs are desirable for labeling cellular organelles. In addition, very small NPs are also more rapidly transported across the endothelium,¹⁵ and it, therefore, may be easier to get a large number of smaller NPs to a specific target than a small number of larger NPs but with the overall mass of magnetic material being the same. Here, we report a novel approach for the synthesis of Co NPs less than 5 nm in diameter, using laser pulses to stimulate the rapid decomposition of cobalt carbonyl in a solution of stabilizers.

* To whom correspondence should be addressed. E-mail: ntk.thanh@ucl.ac.uk. Tel: +44 207-491-6509. Fax: +44 207-629-3569.

[†] Department of Chemistry, University of Liverpool.

[‡] Surface Science Research Centre, University of Liverpool.

^{||} Department of Physics, University of Liverpool.

[⊥] University of New Orleans.

[#] The Royal Institution of Great Britain.

^{\#} University College London.

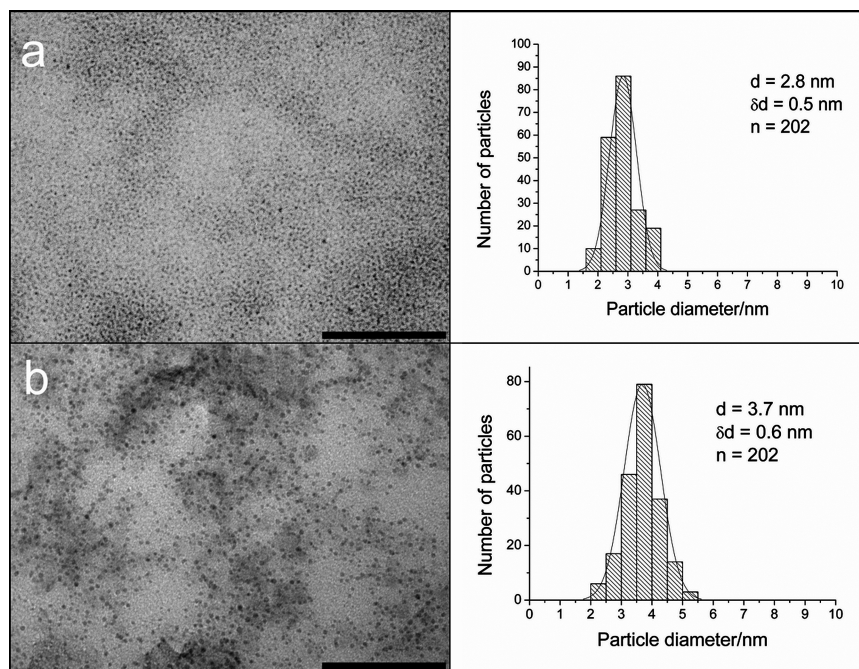


Figure 1. TEM image and size distribution of 2.8 nm Co NPs synthesized using 0.10 M $\text{Co}_2(\text{CO})_8$, 0.04 M OA, and 0.02 M TOPO (a) and of 3.7 nm Co NPs synthesized using 0.10 M $\text{Co}_2(\text{CO})_8$, 0.02 M OA, and 0.04 M TOPO (b) in DCB by irradiation with laser pulses at 266 nm. d = mean particle diameter, δd = standard deviation, n = number of particles measured. Bar 100 nm.

We have chosen to synthesize Co NPs because of scientific and technological interests in utilizing them for biomedical applications. This technique can pave the way for the syntheses of other nanoparticle systems such as Fe–Co, Fe–Pt, and iron oxide.

Experimental Methods

To synthesize Co NPs, a Q-switched Nd:YAG laser (Quantel Brilliant) was used, which produces pulses with a width of 5 ns at a repetition rate of 10 Hz and a wavelength of either 355 or 266 nm. For both wavelengths, the pulse energy was adjusted to 15 ± 3 mJ and the beam diameter to 5 mm. In a typical synthesis, using standard airless conditions, oleic acid (OA, Sigma-Aldrich Inc.) and trioctylphosphine oxide (TOPO, Sigma-Aldrich Inc.) were dissolved in 1,2-dichlorobenzene (DCB, Sigma-Aldrich Inc.) (2 mL) in a 10 mm path length quartz absorption cell (Hellma UK, Ltd.). A solution of $\text{Co}_2(\text{CO})_8$ (Sigma-Aldrich Inc.) in DCB (0.5 mL) was added to the OA/TOPO solution which was then irradiated under vigorous stirring for 30 min. All syntheses were repeated three times and produced consistent results.

Magnetic measurements including zero-field-cooled and field-cooled magnetization were carried out in a MPMS SQUID magnetometer on the diluted samples in DCB. Transmission electron microscopy (TEM) images were acquired using a FEI Tecnai G2 120 kV TEM, and the sizes of NPs were measured using Bersoft Image Standard 5.0 software. Powder X-ray diffractometry (XRD) was carried out using a Panalytical X'Pert system equipped with a graphite monochromator (Co $K\alpha$ radiation, $\lambda = 1.798 \text{ \AA}$). Powder samples were dispersed in absolute ethanol, and then a colloidal solution of NPs was deposited on a Si(100) substrate followed by the natural evaporation of the solvent. The UV–visible spectra of $\text{Co}_2(\text{CO})_8$, DCB, and decane were obtained using a Perkin-Elmer Lambda 25 spectrometer.

Results

Cobalt NPs, with a mean diameter of 2.8 ± 0.5 nm were synthesized by irradiating a solution of 0.10 M $\text{Co}_2(\text{CO})_8$ and

stabilizing ligands (0.04 M OA and 0.02 M TOPO) in DCB with laser pulses at a wavelength of 266 nm (Figure 1a). The obtained Co NPs do not appear to have good contrast in the TEM images due to their low mass–thickness contrast. The obtained Co NPs have very a small diameter (few nanometers), and their electron density is lower than commonly obtained Au NPs. When the concentration of the ligands (0.02 M OA and 0.04 M TOPO) was reversed, while maintaining the same precursor concentration, larger NPs with a mean diameter of 3.7 ± 0.6 nm were produced (Figure 1b). The lower OA concentration means the growing NPs are encapsulated at a slower rate, which results in them having a larger diameter.¹⁷ The stabilizing ligands form a corona on the surface of the NPs, generating steric repulsion, which can prevent aggregation of the NPs due to van der Waals forces. The ligands can also protect the NPs from oxidation. The size of our NPs is comparable with the Co NPs synthesized using laser induced pyrolysis of $\text{Co}_2(\text{CO})_8$ vapor by Zhao et al.;²¹ however, upon annealing in a reducing atmosphere, the latter NPs coalesced to form much larger particles.

The zero-field-cooled (ZFC) and field-cooled (FC) magnetization characterization of the 2.8 nm Co NPs, synthesized as above, are plotted in Figure 2. These NPs have a very low blocking temperature (T_b) of approximately 6 K. The sharp peak in the ZFC curve and the splitting of the ZFC and FC curves close to T_b confirm that the Co NPs have a narrow size distribution.

In order to understand the mechanism of the breakdown of $\text{Co}_2(\text{CO})_8$, the UV–visible spectra of the precursor and DCB were measured. The absorbance spectrum obtained for $\text{Co}_2(\text{CO})_8$ shows absorbance at 266 and 355 nm (Figure 3); the peak near 266 nm can be associated with $\text{Co}_2(\text{CO})_8$ in a bridged form of the molecule and that near 355 nm with $\text{Co}_2(\text{CO})_8$ in a nonbridged form.^{27,28} In contrast, DCB (Figure 3) shows strong absorbance at 266 nm only, resulting in a significant temperature jump following absorption of a short laser pulse, whereas DCB does not absorb light at 355 nm. Irradiation of $\text{Co}_2(\text{CO})_8$ at 266

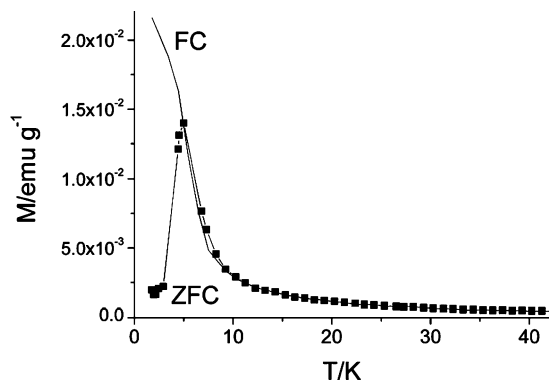


Figure 2. Zero-field-cooled (ZFC) and field-cooled (FC) magnetization curves of the 2.8 nm Co NPs synthesized using 0.10 M $\text{Co}_2(\text{CO})_8$, 0.04 M OA, and 0.02 M TOPO in DCB by irradiation with laser pulses at 266 nm, showing a blocking temperature of 6 K.

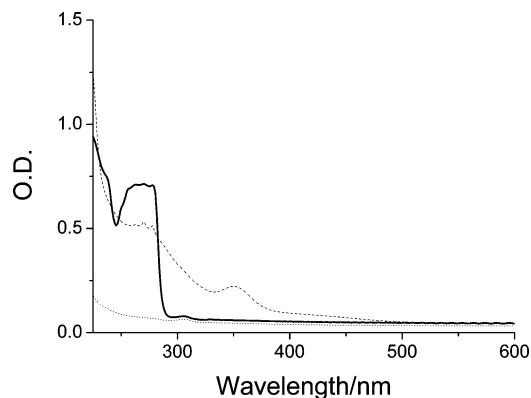


Figure 3. UV-visible absorbance spectrum of $\text{Co}_2(\text{CO})_8$ (0.2 M in decane) (dashed line), DCB (solid line), and decane (dotted line), path length approximately 16 μm .

nm results in the majority of the photolyzed molecules undergoing cobalt–cobalt bond dissociation producing $\text{Co}_2(\text{CO})_7$, while at 355 nm the major process is homolysis of the cobalt–cobalt bond, resulting in two $\text{Co}(\text{CO})_4$ radicals.²⁹ Both species may undergo further decarbonylation, which ultimately may result in the formation of nuclei followed by the growth process of the NPs.³⁰

Since both $\text{Co}_2(\text{CO})_8$ and DCB absorb light at 266 nm, it is unclear if the NPs are being formed by chemical photolysis of the precursor or by pyrolysis caused by localized heating of the solvent. To investigate this, the synthesis was further carried out using laser pulses at 355 nm while the other reaction conditions were kept constant. At this wavelength, only

$\text{Co}_2(\text{CO})_8$ absorbs light but not DCB. Irradiation with laser pulses at this wavelength for 30 min consistently produced Co NPs with a broad size distribution (Figure 4). As a result, in the ZFC curve, beside the peak at around 34 K, we also observed an upturn at very low temperature which could be due to the presence of very small NPs (Figure 5). The splitting between the ZFC and FC data also occurs at a temperature well above the peak at 34 K because of the contribution of relatively large NPs. Powder XRD indicates that the synthesized Co NPs are amorphous, since the pattern is featureless (Figure 6). This is not unexpected, as Co nanoparticles obtained in similar ways have also been found to be amorphous.^{31,32}

Discussion

From the UV–visible absorbance spectra, we determined approximate values of the extinction coefficients of DCB and $\text{Co}_2(\text{CO})_8$ at the relevant wavelengths. This yielded $60 \text{ M}^{-1} \text{ cm}^{-1}$ for DCB at 266 nm,³³ and 1500 and $600 \text{ M}^{-1} \text{ cm}^{-1}$ for $\text{Co}_2(\text{CO})_8$ at 266 and 355 nm, respectively. Using these extinction coefficients, it is possible to estimate the fraction of laser pulse energy absorbed and, thus, the laser pulse-induced temperature increase in the first layer of the sample. For the conditions used here, assuming that all of the absorbed laser pulse energy is rapidly converted to heat, we estimate a temperature increase by approximately $75 \pm 20 \text{ K}$ for excitation at 266 nm, whereas for excitation at 355 nm the maximum temperature increase is only in the order of 5–10 K.

For excitation at 266 nm, the temperature increase occurs to a depth of only a few micrometers and the heat is estimated to dissipate in less than 100 μs .³⁴ We suggest that this rapid temperature increase and decrease is sufficient to cause a short burst of nucleation, followed by a slower growth phase due to rapid diffusion of the sample. Temporal separation of the nucleation and growth phases of particle formation is known to give rise to a population of NPs with a narrow size distribution.³⁵ This could explain why at 266 nm, monodispersed Co NPs are formed.

The average particle size is affected by the length of the growth phase and, thus, by kinetic competition between particle growth and encapsulation of the NPs by OA and TOPO. The NPs produced by pulsed laser irradiation are smaller than those produced by conventional thermal decomposition (8–9 nm) using similar reactant concentrations,³⁶ where the conditions for growth are continuous. Kinetic control of the growth phase also explains the different particle sizes obtained for different ligand concentrations. The percentage yield of the laser synthesis is 3% using the methods described here, which is lower than that obtained by a thermal decomposition method (60%) with

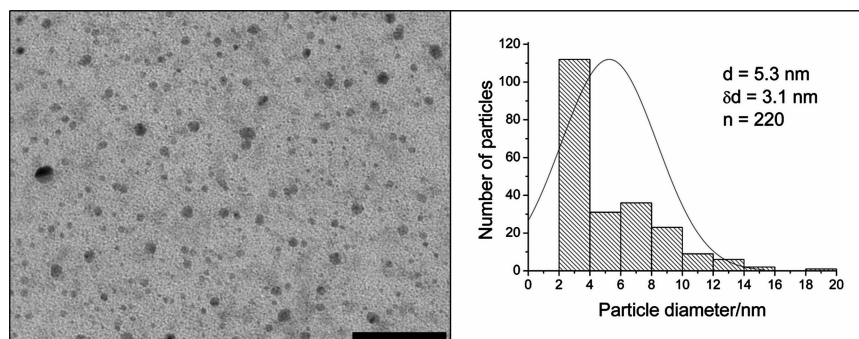


Figure 4. TEM image and size distribution of Co NPs synthesized using 0.10 M $\text{Co}_2(\text{CO})_8$, 0.04 M OA, and 0.02 M TOPO in DCB by irradiation with laser pulses at 355 nm. d = mean particle diameter, δd = standard deviation, n = number of particles measured. Bar 100 nm.

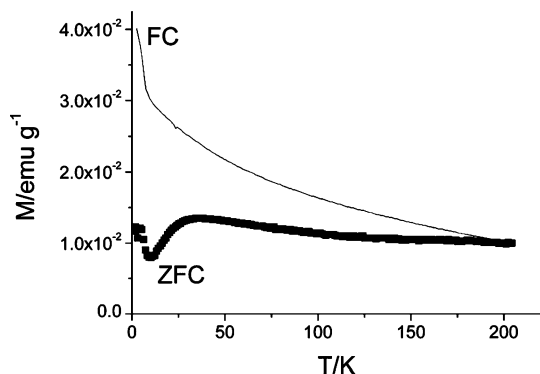


Figure 5. Zero-field-cooled (ZFC) and field-cooled (FC) magnetization curves of Co NPs produced by irradiation of $\text{Co}_2(\text{CO})_8$ at a wavelength of 355 nm in the presence of 0.04 M OA and 0.02 M TOPO.

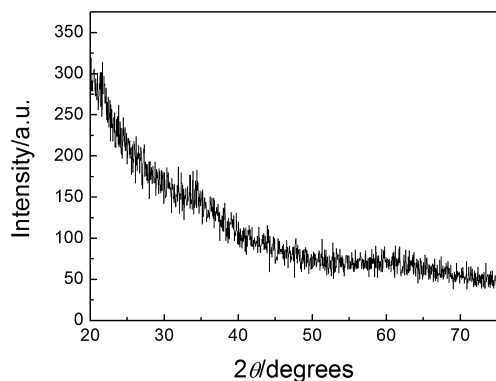


Figure 6. XRD pattern of Co NPs synthesized by the pulse laser irradiation of $\text{Co}_2(\text{CO})_8$, at 355 nm, in the presence of 0.04 M OA and 0.02 M TOPO.

the same reactant concentrations. However, it should be noted that NPs synthesized in the laser experiment are much smaller (2–3 nm) than those obtained by the conventional method (8–9 nm). Therefore, in terms of the number of NPs obtained for a fixed amount of precursor, the yield is very similar. A further increase of the yield of the laser irradiation method could possibly be achieved using a flow system with (magnetic) extraction of NPs and recirculation of the remaining solution. This could be combined with the use of a more powerful laser, allowing irradiation of a larger volume, thus increasing the speed of nanoparticle synthesis.

Laser pulses at 355 nm penetrate to a larger depth, thus affecting a larger volume and yielding a smaller temperature increase, which is insufficient to contribute to the breakdown of $\text{Co}_2(\text{CO})_8$. This means that, at this wavelength, the formation of the NPs is a purely photolytic process. This seems to lead to a longer nucleation phase (possibly limited by the rate of further decarbonylation after formation of the initial photoproduct; see above) and less separation from the growth phase, resulting in the formation of NPs with a broader size distribution. Cobalt NPs do not have an absorption peak at 355 nm;^{37,38} therefore, the broad size distribution of the NPs obtained at this wavelength is unlikely to be a result of annealing, melting, or fragmentation of the synthesized NPs.

Conclusion

In summary, using a novel method of pulsed laser irradiation of $\text{Co}_2(\text{CO})_8$, it has been possible to synthesize small (<5 nm) Co NPs in a solution of DCB. Producing Co NPs of this size is

significant for potential use in biomedical application as their size would allow the rapid renal clearance from the body and, thus, avoid any possible toxic effects of prolonged exposure to Co. The size and the size distribution of the NPs could be controlled by adjusting certain reaction conditions, such as the ligand concentration and the wavelength of light. Adjusting the wavelength of light used to irradiate the precursor also helped to understand the formation mechanism of the Co NPs using this technique. From this, it was deduced that chemical photolysis of $\text{Co}_2(\text{CO})_8$ can produce Co NPs; to synthesize Co NPs with a narrow size distribution, some localized heating of the solvent is required.

Acknowledgment. N.T.K.T. thanks The Royal Society for her University Research Fellowship, and this work was also funded by the Engineering and Physical Sciences Research Council. Ian Prior is thanked for provision of the TEM facilities, and Don Bethell, for useful discussion.

References and Notes

- (1) Alivisatos, A. P. *Science* **1996**, *271*, 933.
- (2) Fendler, J. H. *Chem. Mater.* **1996**, *8*, 1616.
- (3) Rao, C. N. R.; Kulkarni, G. U.; Thomas, P. J.; Edwards, P. P. *Chem. Soc. Rev.* **2000**, *29*, 27.
- (4) Wang, Z. L. *Adv. Mater.* **1998**, *10*, 13.
- (5) El-Sayed, M. A. *Acc. Chem. Res.* **2001**, *34*, 257.
- (6) Roucoux, A.; Schulz, J.; Patin, H. *Chem. Rev.* **2002**, *102*, 3757.
- (7) Lewis, L. N. *Chem. Rev.* **1993**, *93*, 2693.
- (8) Studer, M.; Blaser, H. U.; Exner, C. *Adv. Synth. Catal.* **2003**, *345*, 45.
- (9) Schmidt, H. *Appl. Organomet. Chem.* **2001**, *15*, 331.
- (10) Pankhurst, Q. A.; Connolly, J.; Jones, S. K.; Dobson, J. *J. Phys. D: Appl. Phys.* **2003**, *36*, R167.
- (11) Thanh, N. T. K.; Robinson, I.; Tung, L. D. *Dekker Encyclopedia Nanosci. Nanotechnol.* **2007**, *1*, 1.
- (12) Toda, T.; Igarashi, H.; Uchida, H.; Watanabe, M. *J. Electrochem. Soc.* **1999**, *146*, 3750.
- (13) Maher, B. A. *Magnetic Particle Composition*. Eur. Pat. Appl. WO2006GB0439420061124, May 31, 2007.
- (14) Dobson, J. *Gene Ther.* **2006**, *13*, 283.
- (15) Longmire, M.; Choyke, P. L.; Kobayashi, H. *Nanomedicine* **2008**, *3*, 703.
- (16) Robinson, I.; Alexander, C.; Tung, L. D.; Fernig, D. G.; Thanh, N. T. K. *J. Magn. Mater.* **2009**, *321*, 1421.
- (17) Murray, C. B.; Sun, S. H.; Gaschler, W.; Doyle, H.; Betley, T. A.; Kagan, C. R. *IBM J. Res. Dev.* **2001**, *45*, 47.
- (18) Robinson, I.; Alexander, C.; Lu, L. T.; Tung, L. D.; Fernig, D. G.; Thanh, N. T. K. *Chem. Commun.* **2007**, *44*, 4602.
- (19) Thanh, N. T. K.; Puentes, V. F.; Tung, L. D.; Fernig, D. G. *J. Phys.: Conf. Ser.* **2005**, *17*, 70.
- (20) Lu, L. T.; Tung, L. D.; Robinson, I.; Ung, D.; Tan, B.; Long, J.; Cooper, A. I.; Fernig, D. G.; Thanh, N. T. K. *J. Mater. Chem.* **2008**, *18*, 2453.
- (21) Zhao, X. Q.; Veintemillas-Verdaguer, S.; Bomati-Miguel, O.; Morales, M. P.; Xu, H. B. *Phys. Rev. B: Condens. Matter Mater. Phys.* **2005**, *71*, 024106 1.
- (22) Moras, K.; Schaarschuch, R.; Riehemann, W.; Zinoveva, S.; Modrow, H.; Eberbeck, D. *J. Magn. Mater.* **2005**, *293*, 119.
- (23) Bomati-Miguel, O.; Leconte, Y.; Morales, M. P.; Herlin-Boime, N.; Veintemillas-Verdaguer, S. *J. Magn. Mater.* **2005**, *290*, 272.
- (24) Kurland, H. D.; Grabow, J.; Staupendahl, G.; Andra, W.; Dutz, S.; Bellemann, M. E. *J. Magn. Mater.* **2007**, *311*, 73.
- (25) Wang, C. Y.; Fang, J. Y.; He, J. B.; O'Connor, C. J. *J. Colloid Interface Sci.* **2003**, *259*, 411.
- (26) Mornet, S.; Vasseur, S.; Grasset, F.; Duguet, E. *J. Mater. Chem.* **2004**, *14*, 2161.
- (27) Sweany, R. L.; Brown, T. L. *Inorg. Chem.* **1977**, *16*, 421.
- (28) Abrahamson, H. B.; Frazier, C. C.; Ginley, D. S.; Gray, H. B.; Lillenthal, J.; Tyler, D. R.; Wrighton, M. S. *Inorg. Chem.* **1977**, *16*, 1554.
- (29) Moskovich, S.; Reuvenov, D.; Schultz, R. H. *Chem. Phys. Lett.* **2006**, *431*, 62.
- (30) Privman, V.; Goia, D. V.; Park, J.; Matijevic, E. *J. Colloid Interface Sci.* **1999**, *213*, 36.
- (31) Xie, C. S.; Hu, J. H.; Wu, R.; Xia, H. *Nanostruct. Mater.* **1999**, *11*, 1061.

(32) Kobayashi, Y.; Horie, M.; Konno, M.; Rodriguez-Gonzalez, B.; Liz-Marzan, L. M. *J. Phys. Chem. B* **2003**, *107*, 7420.

(33) Simons, W. W. *The Sadtler Handbook of Ultraviolet Spectra*; Sadtler & Heyden: Philadelphia, PA, 1979.

(34) Wray, W. O.; Aida, T.; Dyer, R. B. *Appl. Phys. B: Lasers Opt.* **2002**, *74*, 57.

(35) Murray, C. B.; Norris, D. J.; Bawendi, M. G. *J. Am. Chem. Soc.* **1993**, *115*, 8706.

(36) Puentes, V. F.; Zanchet, D.; Erdonmez, C. K.; Alivisatos, A. P. *J. Am. Chem. Soc.* **2002**, *124*, 12874.

(37) Creighton, J. A.; Eadon, D. G. *J. Chem. Soc.: Faraday Trans.* **1991**, *87*, 3881.

(38) Chen, G. X.; Hong, M. H.; Lan, B.; Wang, Z. B.; Lu, Y. F.; Chong, T. C. *Appl. Surf. Sci.* **2004**, *228*, 169.

JP9014564